30 September 2019

Solvent-Free Powder Synthesis and Thin Film Chemical Vapour Deposition of a Zinc Bipyridyl-Triazolate Framework

Timothée Stassin[1], Ivo Stassen, Nathalie Wauteraerts, Alexander John Cruz, Marianne Kräuter, Anna Maria Coclite, Dirk De Vos, Rob Ameloot

1. KU Leuven

Abstract

MAF-252, a non-porous crystalline coordination polymer, is obtained from the solvent-free reaction of ZnO with 3-(2-pyridyl)-5-(4-pyridyl)-1,2,4-triazole. MAF-252 can be synthesized in powder form and deposited as thin films, starting from ZnO powder and layers, respectively. Chemical vapour deposition (CVD) of MAF-252 enables conformal and patterned thin films, even on high aspect ratio features.

Keywords

Chemical Vapour Deposition (CVD), Thin Films, Coordination Polymers, Solvent-free reactions

https://doi.org/10.26434/chemrxiv.9916622.v1

Solvent-free powder synthesis and thin film chemical vapour deposition of a zinc bipyridyl-triazolate framework

Timothée Stassin,[a] Ivo Stassen,[a] Nathalie Wauteraerts,[a] Alexander John Cruz,[a] Marianne Kräuter,[b] Anna Maria Coclite,[b] Dirk De Vos,[a] and Rob Ameloot*[a]

Abstract: MAF-252, a non-porous crystalline coordination polymer, is obtained from the solvent-free reaction of ZnO with 3-(2-pyridyl)-5-(4-pyridyl)-1,2,4-triazole. MAF-252 can be synthesized in powder form and deposited as thin films, starting from ZnO powder and layers, respectively. Chemical vapour deposition (CVD) of MAF-252 enables conformal and patterned thin films, even on high aspect ratio features.

Introduction

Coordination polymers are built from metal ion nodes interconnected by organic linkers. Among these materials, crystalline and microporous metal-organic frameworks (MOFs) have been extensively studied because of their record-breaking specific surface area (up to 7500 $m^2 g^{-1}$) and functionalisable pore interior.[1,2] MOFs are typically synthesized under solvothermal conditions. For example, Yaghi and co-workers prepared zeolitic imidazolate frameworks (ZIFs), a subclass of MOFs, using metal salts and various imidazole linkers in solution.[3] At the same time, Chen and co-workers obtained similar or identical materials, and called these metal-azolate frameworks (MAFs).[4,5] Later, a more sustainable preparation method was demonstrated, based on solvent-free reactions in mixtures of metal oxide and linker (OSFR).[6,7] Interestingly, a number of MOF materials can only be obtained under solvent-free conditions.[8]

The deposition of new materials as thin film, a prerequisite for their introduction in several applications (e.g., microelectronics),[9] is often achieved through adaptation of powder preparation routes.[10] For example, MOF chemical vapour deposition (MOF-CVD) was inspired by OSFR chemistry.[11] The MOF-CVD approach relies on two steps: vapour-phase deposition of an oxide precursor followed by its reaction with the vaporised linker.[11–14] Recently, we developed CVD protocols for the microporous zinc 2-methylimidazolate ($[Zn(mIm)_2]$) MAF-4 (also known as ZIF-8) and mesoporous zinc 2-ethylimidazolate ($[Zn(eIm)_2]$) MAF-6.[11,14] Other candidates to expand the scope of this CVD approach are an isostructural series of MAFs based on 3-(2-pyridyl)-5-(4-pyridyl)-1,2,4-triazolate) (Hdpt) or the methylated 3-(3-methyl-2-pyridyl)-5-(4-pyridyl)-1,2,4-triazolate (Hmdpt). These materials have been reported as MAF-25 ($[Co(dpt)_2]$), MAF-26 ($[Co(mdpt)_2]$), MAF-27 ($[Mg(mdpt)_2]$) and MAF-28 ($[Zn(mdpt)_2]$).[6,7] Here, we focused on the undocumented reaction of ZnO with the commercially available linker Hdpt. Surprisingly, the reaction yields a material that is not the Zn-analogue of MAF-25, but rather a novel non-porous crystalline coordination polymer to which we further refer as MAF-252 (read: 'MAF-25 two'). This study reports the solvent-free formation and characterisation of MAF-252 in powder form and as thin films (**Figure 1**).

Results and Discussion

MAF-252 powder was synthesized by heating a mixture of ZnO and Hdpt at 270 °C for 16 h in a glass ampoule, as for the OSFR of other H(m)dpt-based MAFs.[6,7] This approach can be translated to a thin film deposition process following a two-step reaction scheme, as in MOF-CVD: (1) deposition a thin (1-15 nm) ZnO layer and (2) reaction of the ZnO layer with Hdpt vapour. The resulting MAF-252 powder has a beige colour, while the MAF-252 films have a homogeneous mirror-like appearance (**Figure 1**). MAF-252 CVD requires a reaction temperature ≥ 175 °C (step 2) (Figure S3.1). For this study, MAF-252 thin films were deposited within an hour in a simple glass reactor kept at 200 °C to ensure a high enough vapour pressure of this low-volatily linker (Figures

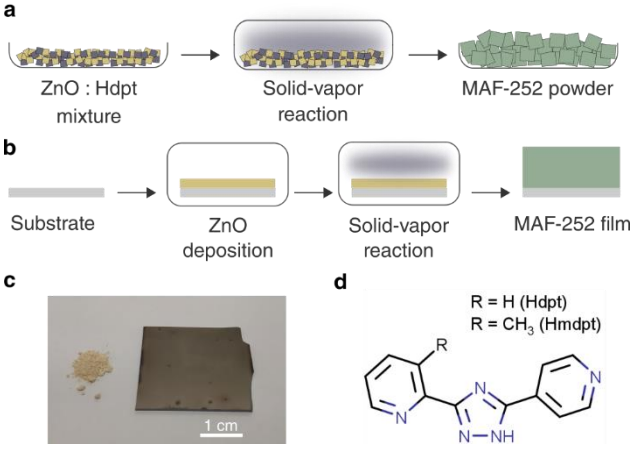

Figure 2. Solvent-free formation of MAF-252 from reaction between ZnO and 3-(2-pyridyl)-5-(4-pyridyl)-1,2,4-triazolate (Hdpt) vapour. a, Schematic representation of the powder synthesis. **b**, Schematic representation of the film deposition. **c**, Image of MAF-252 powder and film. **d**, Chemical structure of Hdpt and Hmdpt.

[a] Timothée Stassin, Dr. Ivo Stassen, Nathalie Wauteraerts, Alexander John Cruz, Prof. Dr. Dirk De Vos, and Prof. Dr. Rob Ameloot
Centre for Membrane Separations, Adsorption, Catalysis and Spectroscopy for Sustainable Solutions (cMACS),
KU Leuven,
Celestijnenlaan 200F box 2454, 3000 Leuven, Belgium.
rob.ameloot@kuleuven.be
www.amelootgroup.org
[b] Marianne Kräuter, Prof. Dr. Anna Maria Coclite
Institute of Solid State Physics
Graz University of Technology
Petersgasse 16, 8010 Graz, Austria.

Supporting information for this article is given via a link at the end of the document.((Please delete this text if not appropriate))

Figure 1

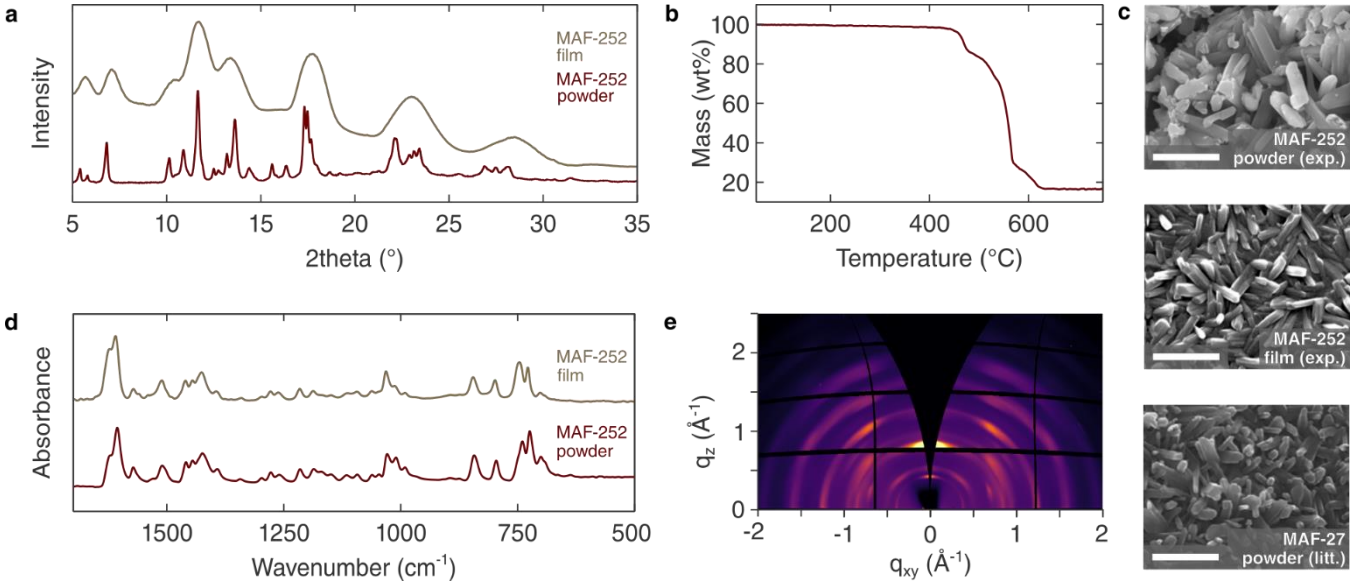

Figure 3. MAF-252 powder and thin films characterisation. a, X-ray diffractogram of MAF-252 powder and film. **b**, TGA of MAF-252 powder. **c**, SEM images of MAF-252 powder, MAF-252 film, and MAF-27 powder reproduced from Ref. 6 with permission from The Royal Society of Chemistry; scale bar = 2 µm. **d**, ATR-FTIR spectra of MAF-252 powder and film. **e**, GIXRD plot of an oriented MAF-252 film grown from (002)-oriented ZnO.

S2.1 and S2.2). MAF-252 CVD is a very simple and robust film deposition process, while ZIF-8 and MAF-6 CVD require precise control over the atmosphere composition (e.g., relative humidity), as well as the temperature gradient between substrate and reactor to achieve reproducible film morphology.[15]

MAF-252 powder and films are crystalline and have similar ATR-FTIR spectra and diffraction patterns (**Figure 2a,d**). No match was found with a known crystal structure. The cell parameters and symmetry cannot be unambiguously identified from the powder pattern because of the limited number of reflections and broad peaks. In both cases, no ZnO is observed by X-ray diffraction, suggesting complete reaction of ZnO with the linker, as also reported for MAF-28.[6]

MAF-252 CVD is sensitive to the ZnO crystallinity and orientation. MAF-252 films grown from amorphous or poorly crystalline ZnO display a powder-like GIXRD pattern, characteristic of a random crystallite orientation (Figure S3.5). Conversely, diffraction spots instead of continuous rings are observed in the GIXRD pattern of MAF-252 films grown from (100)-oriented and (002)-oriented crystalline ZnO layers, suggesting some degree of crystallite orientation (**Figure 2e,** Figure S3.5). These observations are reflected in the film morphology. The morphology of MAF-252 films grown from non-oriented ZnO and powders as observed by SEM is identical and consists of elongated micron-sized crystallites, as for MAF-27 ([Mg(mdpt)$_2$]) (**Figure 2c**).[6] Films grown from oriented ZnO display larger crystallites lying parallel to the surface, that we believe result in the observed out-of-plane orientation in the GIXRD patterns. The formation of these large crystallites likely stems from a difference in MAF-252 nucleation, growth and crystallite ripening for the different types of ZnO precursor, as observed elsewhere for ZIF-8 CVD.[15] MAF-252 CVD is insensitive to the substrate surface chemistry: films with identical morphology can be deposited on Si, Au, and TiO_2 (Figure S3.7).

Thermogravimetric analysis of MAF-252 in air shows no weight loss below 400 °C. (**Figure 2b**). Above 400 °C, the material decomposes to ZnO. Since the observed weight loss (83 %) matches the weight loss expected for [Zn(dpt)$_2$] (84 %), MAF-252 likely has this chemical formula, similar to MAF-25 ([Co(dpt)$_2$]) and MAF-28 ([Zn(mdpt)$_2$]) prepared under the same conditions (Table S4.1).[6,7] Temperature-dependent PXRD and SEM confirm the degradation of MAF-252 above 400 °C (Figures S4.2-S4.4).

While MAF-25 is porous to both N_2 and CO_2, no porosity was detected in MAF-252 powder by N_2 and CO_2 physisorption, and in MAF-252 films by Kr physisorption and MeOH ellipsometric porosimetry, even after activation for 12 h at 350 °C under dynamic vacuum.

MAF-252 CVD was also investigated as a function of starting ZnO thickness and CVD reaction time by SEM, GIXRD, AFM, and ellipsometry. MAF-252 films grown from 1 nm of ZnO show scattered crystals on the surface. Thicker ZnO layers yield MAF-252 films with full surface coverage (Figures S3.2 and S3.3). Conversion of ZnO to MAF-252 is paired with a significant thickness increase. Starting from 1, 4 and 11 nm of ZnO yields MAF-252 films with a thickness of 19, 77, and 109 nm after 16 h, respectively (Figure S3.4). The corresponding film thickness expansion factors are respectively 19, 19 and 10, which is remarkably large for oxide-to-MAF conversions (**Table 1**). As observed for other materials, linker diffusion hindered by the growing film causes incomplete oxide-to-MAF conversion and a lower apparent expansion factor (10 vs 19) when starting from thick oxide layers.[11]

Table 1. MAF structures and corresponding ZnO-to-MAF film expansion factors.

Material	CSD code	Density (g cm^{-3})	Film expansion factor[a]	
			Bulk ZnO	ALD ZnO
ZIF-8 (MAF-4)	VELVOY	0.95	17	12
MAF-6	MECWOH	0.77	22	15
MAF-28	UYAQER	1.53	24	17
MAF-252	This work	-	-	19 (exp.)

[a]Theoretical values based on the bulk ZnO density (5.6 g cm^{-3}) and measured ALD ZnO density (3.9 g cm^{-3}), and the know crystal structure of ZIF-8 (MAF-4), MAF-6, and MAF-28. Experimental value from the ratio of the measured ellipsometric film thickness of ZnO precursor and MAF-252 films.

Different growth stages can be observed: smooth and thin amorphous films in the first 10 min likely corresponding to the surface reaction between ZnO and Hdpt vapour, followed by MAF-252 nucleation and crystallization observed as a steep increase in film thickness and roughness. After 1 h reaction, the growing MAF-252 film hinders the linker diffusion and further oxide conversion. At the same time, larger crystallites are formed by ripening (**Figure 3** and S3.4). A similar growth process was observed for ZIF-8 CVD.[15]

Some applications could benefit from the large film expansion upon conversion of ZnO to MAF-252 and the high carbon content of the resulting films (e.g., carbonization for use in microsupercapacitors). For integration into microelectronics, compatibility of the deposition process with typical microfabrication steps is critical. Therefore, the conformality of MAF-252 CVD and film patterning were evaluated (**Figure 4**). Conformal ZnO precursor layers were deposited by atomic layer deposition (ALD) on high aspect ratio (25:1) silicon micropillars and converted to conformal MAF-252 films over the whole micropillar length. ZnO was also patterned on a flat substrate by lithography and converted to MAF-252. The original pattern was maintained with high fidelity.

Conclusions

The formation of the non-porous crystalline coordination polymer MAF-252 from ZnO and a commercially available linker is an example of the potential of solvent-free, vapour-phase processing. MAF-252 CVD is compatible with microfabrication. While the crystal structure of MAF-252 remains to be solved, its integration in applications could benefit from the robustness and the large film expansion factor of the deposition process.

Experimental Section

Material and methods can be found in the electronic supporting information.

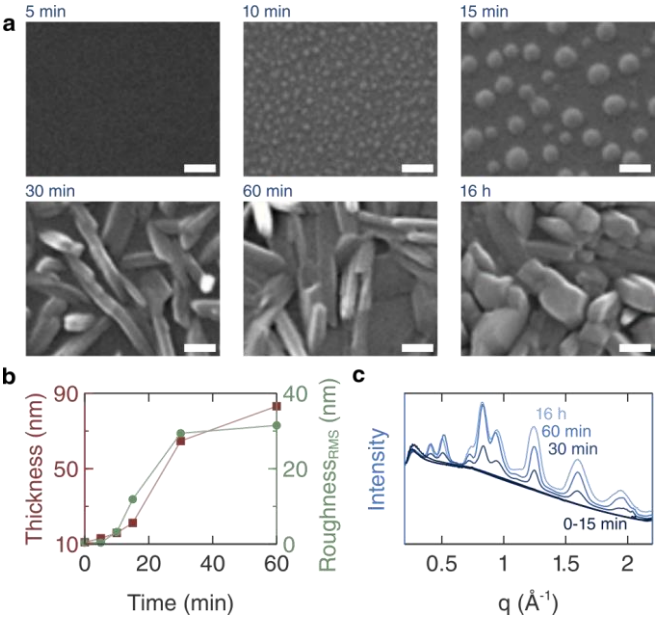

Figure 4. Time evolution of MAF-252 CVD. a, SEM images, **b**, thickness by ellipsometry and RMS roughness by AFM, and **c**, diffractograms extracted from GIXRD patterns of MAF-252 films grown from 10 nm ALD ZnO at various conversion times.

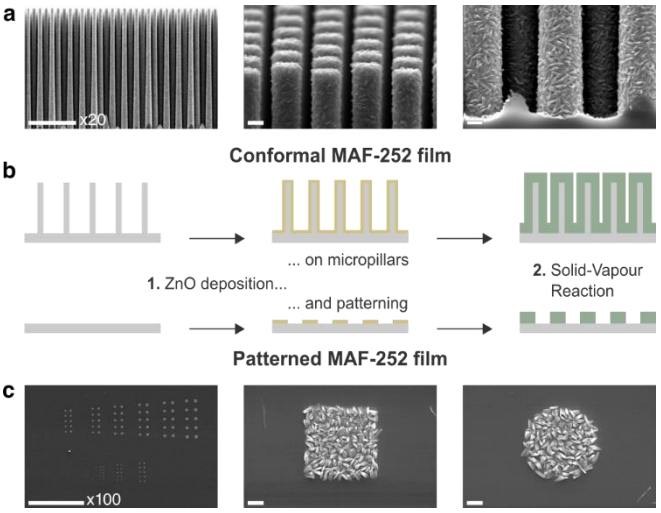

Figure 5. MAF-252 CVD compatibility with typical microfabrication steps. a, SEM images of MAF-252 films deposited conformally on high aspect ratio Si micropillars. **b**, Schematic representation of MAF-252 CVD on high aspect ratio micropillars and film patterning. **c**, SEM images of patterned MAF-252 films; scale bar = 1 µm.

Acknowledgments

T.S., N.W. and I.S. thank the Research Foundation Flanders (FWO) for a SB-PhD fellowship (1S53316N and 1SB7919N) and for a postdoctoral fellowship (and 12L5417N). T.S. is grateful to Roland Resel and Sabina Rodríguez-Hermida for fruitful scientific discussions. R.A. acknowledges the funding from the European Research Council (No. 716472, acronym: VAPORE) and the

Research Foundation Flanders (FWO) for funding in the research projects G083016N, G0E6319N and 1501618N and the infrastructure project G0H0716N. This study is a result from the lead project Porous Materials @ Work (Graz University of Technology, Austria). We acknowledge the Elettra Synchrotron Trieste for allocation of beamtime and thank Luisa Barba and Nicola Demitri for assistance in using beamline XRD1. Min Tu and Helge Reinsch are acknowledged for optimizing the ZnO patterning protocol and for attempting structure refinement, respectively.

Keywords: coordination polymers • chemical vapour deposition • thin films • microfabrication • solvent-free reactions

[1] I. M. Hönicke, I. Senkovska, V. Bon, I. A. Baburin, N. Bönisch, S. Raschke, J. D. Evans, S. Kaskel, *Angew. Chem. Int. Ed.* **2018**, *57*, 13780–13783.
[2] H. Furukawa, K. E. Cordova, M. O'Keeffe, O. M. Yaghi, *Science* **2013**, *341*, 1230444.
[3] K. S. Park, Z. Ni, A. P. Cote, J. Y. Choi, R. Huang, F. J. Uribe-Romo, H. K. Chae, M. O'Keeffe, O. M. Yaghi, *Proc. Natl. Acad. Sci.* **2006**, *103*, 10186–10191.
[4] X.-C. Huang, Y.-Y. Lin, J.-P. Zhang, X.-M. Chen, *Angew. Chem. Int. Ed.* **2006**, *45*, 1557–1559.
[5] A.-X. Zhu, R.-B. Lin, X.-L. Qi, Y. Liu, Y.-Y. Lin, J.-P. Zhang, X.-M. Chen, *Microporous Mesoporous Mater.* **2012**, *157*, 42–49.
[6] J.-B. Lin, R.-B. Lin, X.-N. Cheng, J.-P. Zhang, X.-M. Chen, *Chem. Commun.* **2011**, *47*, 9185–9187.
[7] J.-B. Lin, J.-P. Zhang, X.-M. Chen, *J. Am. Chem. Soc.* **2010**, *132*, 6654–6656.
[8] J. López-Cabrelles, J. Romero, G. Abellán, M. Giménez-Marqués, M. Palomino, S. Valencia, F. Rey, G. Mínguez Espallargas, *J. Am. Chem. Soc.* **2019**, *141*, 7173–7180.
[9] I. Stassen, N. Burtch, A. Talin, P. Falcaro, M. Allendorf, R. Ameloot, *Chem. Soc. Rev.* **2017**, *46*, 3185–3241.
[10] A. Bétard, R. A. Fischer, *Chem. Rev.* **2012**, *112*, 1055–1083.
[11] I. Stassen, M. Styles, G. Grenci, H. V. Gorp, W. Vanderlinden, S. D. Feyter, P. Falcaro, D. D. Vos, P. Vereecken, R. Ameloot, *Nat. Mater.* **2016**, *15*, 304–310.
[12] T. Stassin, S. Rodríguez-Hemida, B. Schrode, A. J. Cruz, F. Carraro, D. Kravchenko, V. Creemers, I. Stassen, T. Hauffman, D. E. D. Vos, et al., *Chem. Commun.* **2019**, *55*, 10056–10059.
[13] M. Krishtab, I. Stassen, T. Stassin, A. J. Cruz, O. O. Okudur, S. Armini, C. Wilson, S. D. Gendt, R. Ameloot, *Nat. Commun.* **2019**, *10*, 1–9.
[14] T. Stassin, I. Stassen, J. Marreiros, A. J. Cruz, R. Verbeke, M. Tu, H. Reinsch, M. Dickmann, W. Egger, I. Vankelecom, et al., *Solvent-Free Powder Synthesis and MOF-CVD Thin Films of the Mesoporous Metal-Organic Framework MAF-6*, **2019**.
[15] A. J. Cruz, I. Stassen, M. Krishtab, K. Marcoen, T. Stassin, S. Rodríguez-Hermida, J. Teyssandier, S. Pletincx, R. Verbeke, V. Rubio-Giménez, et al., *An Integrated Cleanroom Process for the Vapor Phase Deposition of Large-Area Zeolitic Imidazolate Framework Thin Films*, **2019**.